JOURNAL OF MATERIALS SCIENCE **35** (2000) 4809–4814

The effects of drying, aging and curing on an organic - inorganic coating

J. MALZBENDER*, G. DE WITH
Laboratory of Solid State and Materials Chemistry, Eindhoven University of Technology, P.O. Box 513, 5600 MB Eindhoven, The Netherlands
E-mail: J.Malzbender@TUE.NL

The effects of drying, aging and curing on an organic - inorganic coating deposited on float glass substrates were analyzed. Methyltrimethoxysilane was used to immobilize parts of the network connections and silica particles were used as seeds for the nucleation of the gel structure. The coating was produced under acidic conditions to enhance the hydrolysis reaction. The coatings were deposited using a spin-coating technique. The dependence of the elastic modulus, hardness, fracture toughness and residual stress obtained by indentation on the preparation conditions is reported. In addition results obtained by X-ray diffraction (XRD), Atomic Force Microscopy (AFM), X-ray Photon Spectroscopy (XPS) and Infrared-Spectroscopy are analyzed.

1. Introduction

In general, materials can be coated to modify their surface electronic, optical or mechanical properties. In the case of protection against mechanical impact or wear a need for thick coatings exists. The deposition can be performed by various methods, depending on the materials system under consideration. Glass surfaces are often modified by the application of sol – gel coatings, but the preparation of thick coatings by sol – gel processes is hampered by residual stresses that can lead to cracking and delamination [1]. The incorporation of organic groups can reduce the build up of residual stress and therefore aid the preparation of thicker coatings [1].

Sol-gel coatings can be produced by either [2] destabilization of a silica sol, i.e. LUDOX®, or hydrolysis and polycondensation of mixtures in the presence of water. In aqueous solutions no stabilization through steric effects can occur since the particles are not covered by any stabilizing agents and charge effects are negligible, thus colloidal silica particles will aggregate and eventually form clusters [3].

The gelation of a solution involves the polymerisation of monomers to form particles, growth and finally crosslinking of these particles. The crosslinking involves a transport and preferential deposition of silica at the necks between clusters due to the local solubility minimum at the negative radius of curvature. This leads a strengthening of the structure with aging [2].

The viscosity of the liquid determines the thickness that can be acquired in a single deposition step. Further factors influencing the coating in the case of spin coating are the short time for the reacting species to reach an equilibrium configuration, leading to an aggregation process by transport limitation. The structure of the coating is largely determined by the form and composition of the fluid before application. Weakly condensed solutions will easier be contracted leading to smaller pore sizes and higher capillary pressures [4].

The initially included solvents will be removed in a drying process [2]. The structure of the dried coating depends on the competition between the capillary forces, which tend to compress the network, and the condensation reaction, which stiffens the network and leads to an increased hardness [5].

As the structure shrinks some of the bonds will break [6]. Only if the packing density is low no cracking on a microscopic scale will occur. During the collapse new bonds will be formed [2]. In stiffer materials the shrinkage ceases at an earlier stage of drying, causing the pore radius to be larger and the maximum capillary pressure to be smaller [7].

Colloidal particles can be used as nucleation centers for the growth of silica gels [8], thereby increasing the pore size. It has been shown that introducing colloidal particles also increases the strength of the final gel [9]. The disadvantage of this method is the higher curing temperature needed to obtain a dense coating [5]. Furthermore, organics can be used to reduce the connectivity of the network and relax the stress. These organics might be burned out at higher curing temperatures [10].

The drying is followed by a densification or curing, which eliminates the pores and the material can be converted into a glass like structure. The driving force is the surface energy of the porous gel, which eliminates the pores [2].

Independent of the film thickness in plane tensile stresses of the order of 100 MPa [11] can be generated by shrinkage due to the removal of organics or phase changes [12]. Cracking will be observed above a critical thickness [5]. Although flaws lead to failure due to

* Author to whom all correspondence should be addressed.

the local stress, which might be related to a non-uniform pore size, the propagation is due to macroscopic stress [5]. The probability of cracking can be reduced by increasing the fracture toughness of the film, reducing the residual stress, elastic modulus, the fraction of solvent in the film at solidification or the film thickness.

In our experiments organics (methyltrimethoxysilane) were used to immobilize parts of the network connections and silica particles (LUDOX®) were used as seeds for the nucleation of the gel structure. The coating was produced under acidic conditions to enhance the hydrolysis reaction. The coating solutions were aged for different times before application to test the effect of increased aggregation of the structure and solvent evaporation.

2. Experimental

The experiments were carried out using float glass that was coated with an organic-inorganic hybrid coating. The coating fluid contained approximately 30% (weight) solid components, being equal weight amounts of methyltrimethoxysilane (MTMS) and colloidal silica (LUDOX®, average particle size 20 nm), and 70% solvents (2% water, 32% methanol, 1% propanol, 35% glycol). In order to increase the stiffness of the coating, 1 weight% tetraethylorthosilicate (TEOS) was added. The coating fluid was allowed for to pre-react for a time of 60 or 240 minutes.

The rectangular glass substrates of 100 cm^2 were 0.2 cm thick. The substrates were cleaned by scrubbing for 2 minutes using an alkaline soap solution. The soap was removed using flowing water. The glass substrates were then immersed in demineralised water for 1 hour and subsequently dried using nitrogen gas.

The coating fluid was filtered through a 5 μm Millipore© filter before it was applied to the substrate to eliminate any dust particles. The coatings were applied by spinning at speeds between 100 and 2500 rpm in a closed spinner. The closed spinner configuration allowed more homogeneous coatings to be applied. After spinning, the coatings were dried by heating them on a hot plate at 100 °C for one minute. Subsequently, the coatings were cured at 175, 250, 325, 400 and 500 °C for 18 hours or 36 hours. The resulting coating layer thickness was between 1 and 20 μm as measured using profilometry.

Indentation experiments were carried out at room temperature and ambient atmosphere using a home-built instrument. The apparatus permitted up to 25 indentations to be made in one run at loads ranging from 0 to 1000 mN. A Berkovich-type indenter was used. The calibration procedure suggested by Oliver and Pharr [13] was used to correct for the load frame compliance of the apparatus and the imperfect shape of the indenter tip. The load-displacement curves were analyzed using the method proposed by Oliver and Pharr [13], yielding the elastic moduli and the indentation pressure. Radial cracks and spalling of the coating was used to determine the fracture toughness and the residual stress.

Different techniques were used to analyze the morphology of the coatings, i.e. X-ray diffraction (XRD), Atomic Force Microscopy (AFM), X-ray Photon Spectroscopy (XPS) and Infrared-Spectroscopy.

3. Results and discussion

The first section is related to the coating deposition. The subsequent sections summarize and discuss results on the morphology, fracture toughness, residual stress, elastic modulus and hardness of the coatings.

3.1. Deposition

As expected for an evaporating solvent, the thickness of the coating was proportional to $1/\sqrt{\omega}$, where ω is the spin rate. In spin coating the thickness of the coating is balanced between centrifugal force and frictional force [14]. An increase in spin time reduced the coating thickness. This effect was more pronounced for a lower spin rate. The shrinkage of the coating during the curing was larger for a higher curing temperature and decreased with increasing pre-reaction time. Cracking of the coatings was observed above a critical thickness, which is discussed elsewhere [15].

3.2. Morphology

X-ray diffraction showed only a broad diffraction pattern of an amorphous material, which was not analyzed.

The AFM results show that the surface consisted mainly of a crater-like structure, with diameters corresponding to the size of the original LUDOX particles (approximately 20 nm, Figs 1 and 2). Occasionally, larger particles of the order of 100 to 300 nm could be observed on the surface, which were probably related to dust.

Due to the higher thermal expansion coefficient of the coating as compared with the substrate a compressive stress arose in radial direction of the particles and cracks were attracted. However, the elastic modulus and fracture toughness of the silica particles are significantly larger than the modulus and fracture toughness of the matrix and thus cracks cannot penetrate the silica. Instead removal of the particles by poping out of the surface occurred (Fig. 1). The compressive stress around the particles counterbalanced the tensile stress

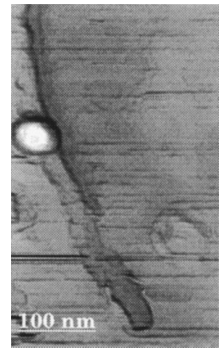

Figure 1 AFM image of the tip of a radial crack showing effects due to crack deflection. The coating of a thickness of 5 μm was cured at 250 °C after a pre-reaction of 1 hour.

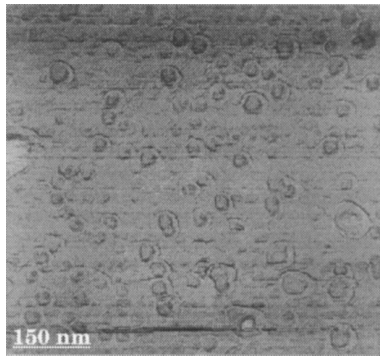

Figure 2 AFM image of the surface of a coating cured at 250 °C (pre-reaction of 1 hour).

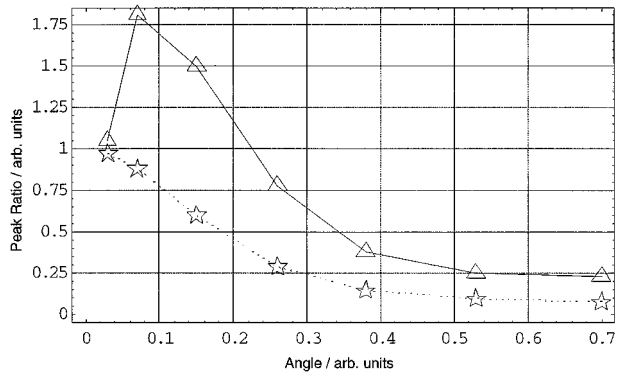

Figure 3 Ratio of the IR-peaks for methyl/water (triangles) and methyl/Si-O (stars) as a function of depth (arbitrary units) of a coating cured at 250 °C after a pre-reaction of 1 hour.

build up by the shrinkage of the matrix, thus leading to a larger critical thickness as compared to a coating without silica addition. Possibly additional stress reduction occurred by bound scission on a microscopic scale.

The XPS revealed a linear decrease of the carbon concentration as a function of depth for coatings cured at 250 °C from 9 at the surface to 7 atomic percent near the interface. Similar for a curing temperature of 175°C the carbon concentration decreased from 10 to 6 atomic percent. For a curing temperature of 400 °C the carbon concentration was independent of depth with an average of 6 atomic percent.

The original solution consisted of a mass ratio of LUDOX to MTMS of 1 : 1. Considering that the LUDOX was in a 50% solution and taking the TEOS addition into consideration, the final atomic concentration of carbon should be approximately 12 at.%. The reduction to 6 at.% observed by XPS can be related to a lower solvent content in the original LUDOX solution due to evaporation, burn-out of CH_3 groups or a not fully cured coating, which increases the relative concentration of oxygen to silicon.

The ratio of the atomic concentration of Si to O for the coating cured at 400 °C was 52%. Considering a fully cured coating this value should be 55%. This suggests that the oxygen concentration was higher than for a fully cured coating, i.e. one Si atom was associated with a larger number of oxygen atoms. This can be explained by less condensation or, considering the results for the lower curing temperatures, burn-out of CH_3 groups.

The higher carbon concentration for the lower curing temperatures and the increase towards the surface can be associated with either an improved curing in the vicinity of the outer atmosphere or residual solvents. The atomic concentrations of C, O and Si were approximately 11%, 57% and 32%, respectively, near the surface and 6%, 62% and 32 %, respectively, near the interface. The carbon concentration and the ratio of the Si to O concentration near the surface were both closer to the theoretically expected values for a fully cured coating, thus suggesting a decrease of the condensation with depth. The total carbon concentration can be related to a competition between condensation and burn out. This is supported by observations on the adhesion of MTMS coatings on steel [16], where a strong adhesion was reported [16] between 200 and 300 °C due to the flexibility of the structure by the remaining Si-CH_3 and Si-OH groups. The adhesion decreased between 300 and 400 °C due to polycondensation of Si-OH bonds.

In order to reveal more details on the curing process IR-spectroscopy was performed on a coating cured at 175 °C. The concentration versus depth of the considered species was estimated by varying the incident angle, since the penetration depth of the light, l, is related to the angle of incidence, α, by: $l \sim 1 - \sin(\alpha)$. Since the instrument was not calibrated for concentrations or depths, only arbitrary units will be used. A peak at 1280 cm^{-1} can be associated with methyl groups in a MTMS – TEOS coating [17]. Furthermore, a peak at approximately 900 cm^{-1} is mainly due to Si-OH [17], whereas a peak at approximately 1100 cm^{-1} can be related to the Si-O bond [18]. The ratio of the IR-peaks for methyl/water and methyl/Si-O as a function of depth in arbitrary units is shown in Fig. 3. Whereas the number of CH_3 groups seems to decrease with depth, similar to the XPS results, the ratio of CH_3 to OH showed a minimum near the surface superimposed to a general decrease with depth. This implied a higher OH concentration, which might be due to the in diffusion of water.

3.3. Fracture toughness

The fracture toughness was calculated using radial cracks and chipping of the coating after indentation [19]. An effect of the layer thickness onto either the fracture toughness or the residual stress could not be confirmed from the indentation measurements in these coatings [19]. The coating porosity and structure will be influenced by the pre-reaction time, but it can be expected that the higher curing temperature leads to a coating of higher density and higher fracture toughness [4]. The fracture toughness increased with curing temperature up to 250 °C, thereafter it was approximately constant (Fig. 4). The fracture toughness (average 0.18 MPa $\cdot$ $m^{0.5}$ [19]) was lower than for dried TEOS gels (0.5 MPa $\cdot$ $m^{0.5}$ [20]). The ratio of the hardness to the fracture toughness (5.4 to 9 $\mu m^{-0.5}$), as an indicator of brittleness, was higher than for dried TEOS gels (3.3 $\mu m^{-0.5}$ [21]).

Our indentation experiments have shown a larger load of delamination for coatings cured at 250 °C after

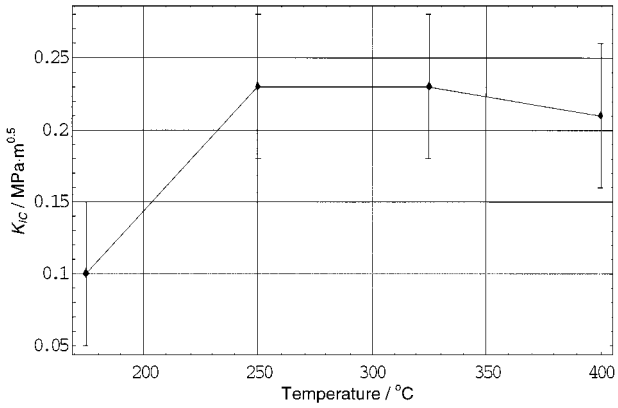

Figure 4 Fracture toughness as a function of the curing temperature (pre-reaction 1 hour).

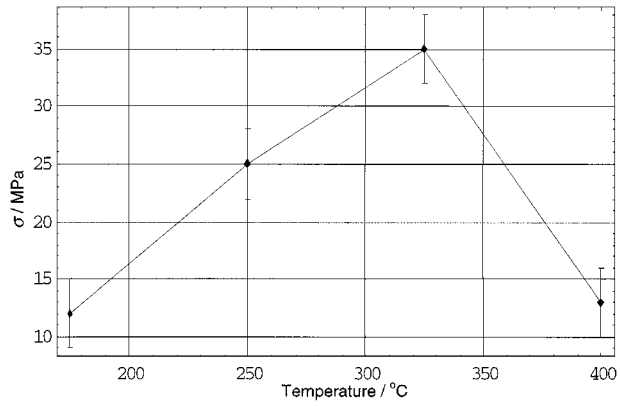

Figure 6 Stress as a function of the curing temperature for a pre-reaction time of 1 hour.

a pre-reaction time of on hour than for coatings cured after a longer pre-reaction time or at a higher curing temperature. This can be related to the higher quantity of uncondensed silanol groups in the fresh solution [22].

3.4. Residual stress

Stresses in the coating will be generated by the drying process and on cooling due to the mismatch in thermal expansion coefficient. The residual stress was calculated using the dependence of the length of radial cracks on the applied load after indentation [19]. The residual stress in the coatings decreased with hydrolysis/pre-reaction time (Fig. 5). An increase of the curing temperature resulted in an increase of the residual stress up to a temperature of 325 °C (Fig. 6). The residual stress decreased at higher temperatures. A similar decrease of the residual stress at higher temperatures has been found for phosphosilicate sol-gel films [23].

Assuming that the stress was due to differences in the thermal expansion coefficient it is possible to calculate the thermal coefficients expansion from the linear increase with temperature up to 325 °C [19]. Using a thermal expansion coefficient of float glass a value of 8.5×10^{-6}/ K [24] a value of 20×10^{-6}/ K results.

The higher residual stress for the fresh coatings (Fig. 5) can be related to the higher concentration of solvents in the initial solution, which resultes in a higher surface tension and capillary pressure as well as a larger reduction of the quantity of residual solvents on curing [14]. The stress is lower for a longer hydrolysis time because of the lower solvent concentration and the increased interlinkage between the particles in the solution [2, 25]. The addition of TEOS leads to a less deformable structure and to the growth of three dimensional oligomers, due to the different hydrolysis – condensation rate as compared to MTMS and SiO_2 – microdomains [26].

Our investigations on the delamination of thick films [15] revealed that delaminated films approach a concave shape, i.e. the edges of delaminated areas were bending away from the substrate. This implies a higher tensile stress in the surface of the coating. The XPS measurements have shown a larger carbon concentration near the surface for coatings cured at a lower temperature, which can be related to a faster curing at the surface. This inhomogeneous curing gives also rise to a larger residual stress near the surface.

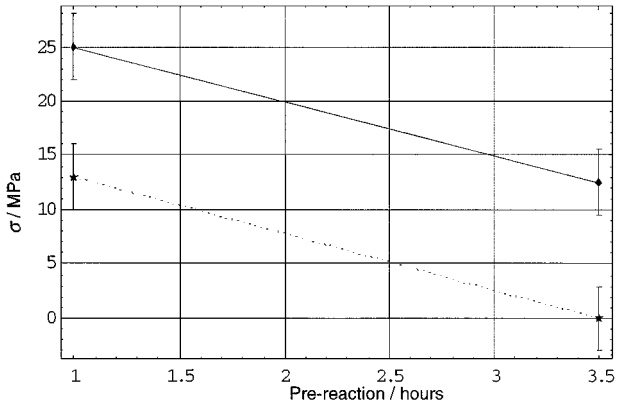

Figure 5 Stress as a function of pre-reaction time. (Dashed line 400 °C, Full line 250 °C)

3.5. Elastic modulus

The elastic modulus did not show a significant dependency on the hydrolysis / pre-reaction time or curing temperature ($E \cong 10$ GPa [19] similar to dried TEOS gels [21]). The dependence of the elasticity onto the indentation depth could be described by models by Doerner [27] or Gao [28]. For details of these measurements and accompanying analysis we refer to [19].

3.6. Hardness

The hardness was determined by indenatation from the maximum load and the contact depth [19]. The hardness showed a maximum near the surface, which decreased to reach a constant level in the "bulk" of the coating. The "bulk" hardness of the coatings increased with curing time and temperature (Table I), similar to results obtained by Izumi *et al.* [29] for MTES coatings on sheet steel. Based on Fourier-transformed infrared spectroscopy Izumi *et al.* [29] concluded that the strengthening of MTMS coatings with increasing temperature was due to the formation of Si-O-Si networks by the polycondensation of Si-OH groups. A condensation reaction was supposed to lead to structural rearrangement up to 300 °C and decomposition of methyl groups should start above this temperature [29].

TABLE I "Bulk" coating hardness in GPa

		Temperature / °C				
Curing time	Pre-reaction	175	250	325	400	500
18 hours	1 hour	1.25	1.25	1.2	1.2	6
18 hours	3.5 hours	——*	1.2	——*	1.5	6
36 hours	1 hour	1.4	——*	1.6	——*	——*

*samples were not produced for this condition.

The limited resolution of the instrument did not allow an accurate estimate of the hardness peak near the surface in our investigations [19]. The rate of decrease of this peak was higher for a longer hydrolysis time but more pronounced for a higher curing temperature [29]. The hardness peak near the surface did not depend on the coating layer thickness. Results on the "bulk" coating hardness after curing at 400 °C have shown an increase with aging of the solution from 1.2 GPa to 1.5 GPa (Table I), which can be associated with network stiffening [4].

The hardness was influenced by the curing time, i.e. the depth of the surface peak reduced by a factor of 2 after a curing of 36 hours at 175 °C and the hardness of the "bulk" coating increased from 1.25 to 1.4 GPa and for 325 °C from 1.2 to 1.65 GPa (Table I). A surface layer probably has formed in the initial stages of the curing process due to the formation of Si-O-Si bonds and is then reduced by equilibration of the OH or CH_3 concentration or the hardness of this layer is reduced by bond scission due to the increasing shrinkage and stress in the structure. The increase in "bulk" coating hardness with curing time might also be related to a reduction of the carbon concentration due to burn out (see section morphology).

The hardness peak near the surface decreased faster for fresh coatings and higher curing temperatures. The inner part of the coating was harder for a longer pre-reaction time and a higher curing temperature. This suggests that the effect responsible for this behavior was more dominant for longer pre-reaction time, but decreases with curing temperature. Similar observations have been reported for TiO_2 sol – gel coatings [30] and were related by X – ray diffraction and XPS measurements to formation of an Anatase – like or crystalline structure. In agreement with our observations [19] the softer inner layer might possess a higher OH concentration (section 3.4) [30]. Since our X – ray diffraction measurements could not reveal a crystalline structure near the surface, nor was this possible in other reports [31], it is assumed along with Fabes *et al*. [16], that this top layer has a structure similar to amorphous silica.

A relationship between the hardness peak and the concentration difference a diffusion of the concentration of OH, carbon or CH_3 appears possible. Thus, in addition to the out – diffusion from the surface layer, which is in fact a depletion mechanism, the diffusion from the bulk of the coating to the surface has to be taken into consideration.

XPS measurements of the carbon concentration in these layers revealed a nearly linear decrease with increasing sputtering depth (Section 3.3), which is opposite to general expectations. Thus the observed hardness peak might be related to decreasing number of non-reacted OH bonds.

Coatings cured at 500 °C showed glass-like properties, e.g. a very high elastic modulus of approximately 70 GPa and a hardness of approximately 6 GPa, which suggests that CH_3 groups have been burned out. This is in agreement with observations on MTMS coatings on steel where such burn out between 400 and 500 °C has been reported [32].

The hardness peak near the surface was reduced after 46 days aging of the cured coating [19]. The "bulk" hardness of the coating was preserved. The surface peak hardness was reduced by 25 to 75% for 250 °C and 50% for 400 °C. The reduction was stronger for the strained Si-O-Si bonds in 250 °C cured coatings, which also had a larger depth of the initial surface peak. Prolonged exposure to the atmosphere can lead to degradation of Si – O groups [33] and so change the surface hardness of the coating.

It can be suggested that repetitive deposition of thin films might lead to a film harder than produced for similar curing temperature and condensation time by a single deposition due to the multiplicity of high hardness surface layers, but requires a curing after each deposition [34].

4. Conclusion

The dependence of the fracture toughness, elastic modulus and hardness of a sol - gel coating onto curing temperature and pre-reaction time can be explained on the basis of different reactivity, residual stress, changes in the structure of the solution with aging time and the mismatch in thermal expansion coefficient.

Acknowledgement

The authors would like to acknowledge dr. J. M. J. den Toonder, dr. A. R. Balkenende and dr. T. N. M. Bernards (Philips Research Laboratories, Eindhoven, The Netherlands) for their technical support and useful discussions.

References

1. N. TOHGE, K. TADANAGA, H. SAKATANI and T. MINAMI, *J. Mater. Sci. Lett.* **15** (1996) 1517.
2. J. ZARZICKI, M. PRASSAS and J. PHALIPPOU, *ibid.* **17** (1982) 3371.
3. P. W. J. G. WIJNEN, T. P. M. BEELEN, K. P. J. RUMMENS, H. C. P. L. SAEIJS, J. W. DE HAAN, L. J. M. VAN DE VEN and R. A. VAN SANTEN, *J. Colloid Interf. Sci.* **145** (1991) 17.
4. G. W. SCHERER, *J. Non-Cryst. Solids* **147/148** (1992) 363.
5. T. KAWAGUCHI, H. HISHIKURA and J. IURA, *ibid.* **100** (1988) 220.
6. T. KAWAGUCHI, J. IURA, N. TANEDA, H. HISHIKURA and Y. KOKUBA, *ibid.* **82** (1986) 50.
7. G. W. SCHERER, S. A. PARDENEK and R. W. SWIATEK, *ibid.* **107** (1988) 14.
8. J. ZARZICKI, *ibid.* **100** (1988) 359.
9. R. D. SHOUP, *Colloid and Interface Science* **3** (1976) 63, M. Toki, *ibid.* **100** (1988) 479.

10. H. OKAZAKI, T. KITAGAWA, S. SHIBATA and T. KIMURA, *ibid.* **116** (1990) 87.
11. J. DUMAS, J. F. QUINSON and J. SERUGETTI, *ibid.* **125** (1990) 244.
12. H. SCHMIDT, R. RINN, R. NASS and D. SPORN, *Mater. Res. Soc. Symp. Proc.* **121** (1988) 743.
13. W. C. OLIVER and G. M. PHARR, *J. Mater. Res.* **7** (1992) 1564.
14. C. J. BRINKER, A. J. HURD, P. R. SCHUNK, G. C. FRYE and C. S. ASHLEY, *J. Non-Cryst. Solids* **147/148** (1992) 424.
15. J. MALZBENDER and G. DE WITH, *Thin Solid Films* **359** (2000) 210.
16. B. D. FABES and W. C. OLIVER, *J. Non-Cryst. Solids* **121** (1990) 348.
17. A. MATSUDA, Y. MATSUNO, M. TATSUMISAGO and T. MINAMI, *J. Am. Ceram. Soc.* **81** (1998) 2849.
18. R. M. ALMEIDA and C. G. PANTANO, *J. Appl. Phys.* **68** (1990) 4225.
19. J. MALZBENDER, J. M. J. DEN TOONDER and G. DE WITH, *Thin Solid Films* **366** (2000) 139.
20. D. E. BORNSIDE, C. W. MACOSKO and L. E. SCRIVEN, *J. Appl. Phys.* **66** (1989) 5185.
21. Y. HOSHINO and J. D. MACKENZIE, *J. Sol-Gel Sci. Tech.* **5** (1995) 8.
22. T. NAKANO and T. OHTA, *J. Electrochem. Soc.* **142** (1995) 918.
23. R. R. A. SYMS, *J. Non-Cryst. Solids* **167** (1994) 16.
24. Product Information, Precision Glass & Optics, Santa Ana, California, USA, 1999.
25. T. HORIUCHI, T. SUGIYAMA, K. MIZUNO, T. OSAKI, K. SUZUKI, S. TOMURA and T. MORI, *J. Ceram. Soc. Jpn.* **104** (1996) 1135.
26. C. DELLA VOLPE, S. DIRE and E. PAGANI, *J. Non-Cryst. Solids* **209** (1997) 51.
27. M. F. DOERNER and W. D. NIX, *J. Mater. Res.* **1** (1986) 6501.
28. H. GAO, C. H. CHIU and J. LEE, *Int. J. Solids Structures* **29** (1992) 2471.
29. K. ISUMI, H. TANAKA, Y. UCHIDA, N. TOHGE and T. MINAMI, *J. Non-Cryst. Solids* **147/148** (1992) 483.
30. H. HIRASHIMA and T. KUSAKA, *Sol-Gel Optics II* **1758** (1992) 67.
31. H. IMAI, H. MORIMOTO, A. TOMINAGA and H. HIRASHIMA, *J. Sol-Gel Sci. Tec.* **10** (1997) 4.
32. A. SAKAR, Y. YAN, P. D. FUQUA and W. JAHN, *Mater. Res. Soc. Symp. Proc.* **435** (1996) 351.
33. R. DI MAGGIO, R. CAMPOSTRINI and G. CARTURAN, *J. Mater. Sci. Lett.* **14** (1995) 1591.
34. R. MIZUTANI, Y. OONO, J. MATSUOKA, H. NASU and K. KAMIYA, *J. Mater. Sci.* **29** (1994) 5773.

Received 20 September 1999
and accepted 2 March 2000